



Heriot-Watt University
Research Gateway

Inflammatory responses of a human keratinocyte cell line to 10 nm citrate- and PEG-coated silver nanoparticles

Citation for published version:

Bastos, V, Brown, DM, Johnston, HJ, Daniel-da-Silva, AL, Duarte, IF, Santos, C & Oliveira, H 2016, 'Inflammatory responses of a human keratinocyte cell line to 10 nm citrate- and PEG-coated silver nanoparticles', *Journal of Nanoparticle Research*, vol. 18, 205. <https://doi.org/10.1007/s11051-016-3515-x>

Digital Object Identifier (DOI):

[10.1007/s11051-016-3515-x](https://doi.org/10.1007/s11051-016-3515-x)

Link:

[Link to publication record in Heriot-Watt Research Portal](#)

Document Version:

Peer reviewed version

Published In:

Journal of Nanoparticle Research

Publisher Rights Statement:

The final publication is available at Springer via <http://dx.doi.org/10.1007/s11051-016-3515-x>

General rights

Copyright for the publications made accessible via Heriot-Watt Research Portal is retained by the author(s) and / or other copyright owners and it is a condition of accessing these publications that users recognise and abide by the legal requirements associated with these rights.

Take down policy

Heriot-Watt University has made every reasonable effort to ensure that the content in Heriot-Watt Research Portal complies with UK legislation. If you believe that the public display of this file breaches copyright please contact open.access@hw.ac.uk providing details, and we will remove access to the work immediately and investigate your claim.

1 **Inflammatory responses of a human keratinocyte cell line to 10 nm**
2 **citrate- and PEG-coated silver nanoparticles**

3 Bastos V.¹, Brown D.², Johnston H.², Daniel-da-Silva, A.L.³, Duarte I.F.³, Santos C.^{1,4} and
4 Oliveira H.¹

5

6 ¹*CESAM & Laboratory of Biotechnology and Cytomics, University of Aveiro, 3810-193 Aveiro, Portugal*

7 ²*School of Life sciences, Heriot-Watt University, Riccarton, Edinburgh EH14 4AS, UK*

8 ³*CICECO – Aveiro Institute of Materials, Department of Chemistry, University of Aveiro, 3810-193 Aveiro, Portugal*

9 ⁴*Department of Biology & Greenup / Citab -UP, Faculty of Sciences, University of Porto, Rua do Campo Alegre, Porto*

10

11 *corresponding author: csantos@fc.up.pt

12

13 **Abstract**

14 Silver nanoparticles (AgNPs) are among the most commonly used engineered NPs and various
15 commercially available products are designed to come in direct contact with the skin (wound
16 dressings, textiles, creams, among others). Currently, there is limited understanding of the
17 influence of coatings on the toxicity of AgNPs and in particular their ability to impact on AgNP's
18 mediated inflammatory responses. As AgNPs are often stabilized by different coatings, including
19 citrate and polyethyleneglycol (PEG), in this study we investigate the influence of citrate (Cit10)
20 or PEG (PEG10) coatings to 10 nm AgNP on skin, using human HaCaT keratinocytes. AgNPs
21 cytotoxicity and inflammatory response (nuclear factor (NF)- κ B induction and cytokine
22 production) of HaCaT were assessed after *in vitro* exposure to 10 μ g/mL and 40 μ g/mL after 4,
23 24 and 48 h. Results showed that although both types of coated AgNPs decreased cell proliferation
24 and viability, Cit10 AgNPs were more toxic. NF- κ B inhibition was observed for the highest
25 concentration (40 μ g/mL) of PEG10 AgNPs, and the putative link to early apoptotic pathways
26 observed in these cells is discussed. No production of IL-1 β , IL-6, IL-10 and TNF α was stimulated
27 by AgNPs. Furthermore, Cit10 and PEG10 AgNPs decreased the release of MCP-1 by HaCaT
28 cells after 48 h of exposure. As cytokines are vital for the immunologic regulation in the human
29 body, and it is demonstrated that they may interfere with NPs, more research is needed to
30 understand how different AgNPs affect the immune system.

31

32 **Introduction**

33 Nanotechnology-based consumer products are exponentially increasing, being nanosilver-
34 containing products among the most commonly used (Vance et al., 2015). Silver nanoparticles
35 (AgNPs) are widely used due to their enhanced physicochemical properties and biological
36 activities such as their antimicrobial activity. Their applications range from medicine and industry
37 to household and personal care products (EPA, 2010) or clothing (Abdelhalim and Jarrar, 2011;
38 Behra et al., 2013; Benn and Westerhoff, 2008; Eckhardt et al., 2013; Nowack et al., 2011). The
39 increased exploitation of AgNPs and consequent release into the environment raises concerns
40 about their possible impacts on the environment and on human health (Nowack and Bucheli,
41 2007). There is an array of AgNPs that are being exploited, which vary with respect to their
42 physicochemical properties (e.g. size, shape, charge, surface coating, dispersion state) (Ahlberg
43 et al., 2014; Boonkaew et al., 2014; Comfort et al., 2014; Kim et al., 2012; Park et al., 2011b).
44 Existing studies have demonstrated that the physicochemical properties of AgNPs are able to
45 influence their toxicity for different cell lines [eg., human keratinocytes (HaCaT and primary
46 keratinocytes), normal fibroblasts (NHF), rat adrenal pheochromocytoma (PC12), and mouse
47 osteoblasts (MC3T3-E1), fibroblasts (L929) and macrophages (RAW 264.7)]. However, little
48 attention has been given to the coating-dependent toxicity of AgNPs. Thus, research on the

49 toxicity of AgNPs of varied physicochemical properties is critical in order to better predict the
50 risks they pose.

51 It has been reported that nanoparticle coating, media composition and ionic strength influence the
52 surface chemistry, shape, aggregation state and dissolution of AgNPs, which in turn can
53 differently affect their cellular uptake and biological effects (Tejamaya et al., 2012). Indeed, a
54 few studies addressing the uptake (by embryonic fibroblasts NIH/3T3, keratinocytes HaCaT and
55 hepatoma cells Hepa-1c1c7, respectively) of different coated AgNPs and their influence on
56 cytotoxicity have been reported (Caballero-Díaz et al., 2013; Lu et al., 2010; Pang et al., 2015).
57 Citrate is the most commonly used reducing and stabilizing agent of AgNPs, rendering NPs with
58 a negative surface charge and providing colloidal stability through electrostatic repulsions
59 (Sharma et al., 2009). Among other coating agents of AgNPs, low molecular weight
60 polyethyleneglycol (PEG), which stabilizes AgNPs through steric interactions, has been
61 increasingly used in biomedical applications as it enhances biocompatibility and increases blood
62 circulation time (Ginn et al., 2014; Ryan et al., 2008).

63 Assessment of the ability of NPs to induce inflammatory responses is commonly used as an
64 indicator of toxicity. For example, Chalew and Schwab (2013) studied the inflammatory effects
65 of AgNPs, titanium dioxide (TiO₂NPs), and zinc oxide (ZnONPs) (0, 0.1, 1, 10, and 100 mg/L)
66 on human intestinal Caco-2 and SW480 cells and found that all NPs increased IL-8 cytokine
67 generation in both cell lines. Also, Park et al (2011a) observed that pro-inflammatory cytokines
68 (IL-1, TNF- α , and IL-6) and Th0 cytokine (IL-2) were progressively increased by day 28 after a
69 single intratracheal instillation of AgNPs in mice. Suliman and co-workers (2013b) found that
70 50 μ g/mL AgNPs exposure to human lung epithelial (A549) cells significantly increased the level
71 of pro-inflammatory cytokines, namely interleukin-1 β (IL-1 β) and interleukin-6 (IL-6). Yang and
72 collaborators also observed IL-1 β release by human blood monocytes in response to AgNPs
73 (Yang et al., 2012). However, Wong et al (2009) found an anti-inflammatory effect of AgNPs to
74 two mouse macrophage cell lines, RAW264.7 and J774.1, where AgNPs blocked TNF- α
75 production. On the other hand, we could not find studies reporting the induction of anti-
76 inflammatory cytokines after exposure to NPs (Murray et al., 2013; Orłowski et al., 2013;
77 Samberg et al., 2009). Cytokines can strongly activate inflammatory responses and cell death in
78 various tissues, including the skin (Fujiwara and Kobayashi, 2005; Graves et al., 2004). Indeed,
79 a study on the effects of UVB radiation using HaCaT cells reported an increase of various pro-
80 inflammatory cytokines - interleukin (IL)-1 β IL-6, IL-8, interferon (IFN)- γ , granulocyte-colony
81 stimulating factor (G-CSF), macrophage inflammatory protein (MIP)-1 β , and tumor necrosis
82 factor (TNF)- α (Yoshizumi et al., 2008). Murray et al (2013) found increased IL-8 and IL-6 in
83 human epidermal keratinocytes (HEK cells) after exposure to superparamagnetic iron oxide
84 (SPION) NPs (2.6, 5.2, 13, and 26 μ g/cm² for 24 h). In other study using HEK cells, quantum dot
85 NPs significantly increase IL-6 at 1.25 nM to 10 nM, while IL-8 increased from 2.5 nM to 10nM

86 after 24 h and 48 h (Zhang et al., 2008). Therefore, as products containing AgNPs can be applied
87 to the skin (e.g. wound dressing), and as there are experimental evidences for skin penetration of
88 25 ± 7 nm AgNPs (also in intact skin) (Larese et al., 2009) and 20 – 40 nm AgNPs (George et al.,
89 2014), the human keratinocyte cell line HaCaT was selected as an *in vitro* model in this study. It
90 is well known that cytokines play crucial roles in immunologic regulation in the human body and
91 are involved in the induction of proliferation, differentiation, and cell death in many cell types
92 (Yarilin and Belyakov, 2004). Moreover, activation of the transcription factor nuclear factor
93 kappa B (NF- κ B) has been shown to play a central role in the enhanced expression and regulation
94 of cytokine genes (Kelso, 1998). There is also evidence that carbon NPs can activate NF- κ B in
95 macrophages which stimulates TNF α production (Brown et al., 2004). To our knowledge, the
96 activation of NF- κ B in keratinocytes has not been studied previously.

97 In our previous study (Bastos et al., 2016) we evaluated the toxicity of 30 nm AgNPs coated with
98 citrate or PEG on HaCaT cells. Our results showed that Cit30 AgNPs were more cytotoxic than
99 PEG30 AgNPs. Concerning cytokine release, both Cit30 and PEG30 AgNPs induced a decrease
100 in MCP-1 production but no effect on other cytokines, namely IL-1 β , IL-6, IL-10 and TNF- α
101 (Bastos et al, 2016).

102 In this study, we aimed to compare the inflammatory responses of HaCaT cells exposed to well-
103 characterized 10 nm AgNPs coated with citrate or PEG, in order to explore the influence of
104 smaller sizes of AgNPs on the inflammatory response. In particular, the effects on viability,
105 expression of the pro-inflammatory transcription factor NF- κ B and production of cytokines such
106 as interleukin-1 beta (IL-1 β), IL-6, tumour necrosis factor-alpha (TNF- α), IL-10 and monocyte
107 chemoattractant protein-1 (MCP-1) were assessed.

108

109 **Material and methods**

110 *Chemicals*

111 Sterile, purified and endotoxin-free silver nanoparticles (Biopure AgNPs 1.0 mg/mL in water),
112 with a diameter of 10 nm and a citrate or polyethyleneglycol (PEG) surface, designated as Cit10
113 and PEG10, respectively, were purchased from Nanocomposix Europe (Prague, Czech Republic).
114 Dulbecco's modified Eagle's medium (DMEM), fetal bovine serum (FBS), antibiotics and
115 phosphate buffer saline (PBS, pH 7.4) were purchased from Life Technologies (Carlsbad, CA,
116 USA). 3-(4,5-dimethylthiazol-2-yl)-2,5-diphenyltetrazolium bromide (MTT), Mowoil and DAPI
117 were obtained from Sigma-Aldrich (St. Louis, MO, USA).

118

119 *Physicochemical characterization of AgNPs*

120 The morphology and size of AgNPs were assessed by transmission electron microscopy (TEM)
121 using a transmission electron microscope Hitachi H9000 NAR (Hitachi High-Technologies
122 Europe GmbH, Germany) operating at 300 kV. Samples for TEM analysis were prepared by

123 evaporating dilute suspensions of AgNPs on a copper grid coated with an amorphous carbon film.
124 The hydrodynamic diameter and polydispersity index (Pdl) were measured by dynamic light
125 scattering (DLS) and the zeta potential was assessed by electrophoretic mobility, both
126 measurements using a Zetasizer Nano ZS (Malvern Instruments, UK). Silver quantification
127 measurements were performed by inductively coupled plasma optical emission spectrometry
128 (ICP-OES) in an Activa M Radial spectrometer (Horiba Jobin Yvon), employing a charge coupled
129 device (CCD) array detector, with a wavelength range of 166–847 nm and radial plasma view.
130 Samples for ICP-OES were prepared by addition of 10 μ L AgNPs (1.0 mg/mL) to 990 μ L of
131 either ultrapure water or complete culture medium, incubated for 0, 4, 24 or 48h, then centrifuged
132 at 40000 rcf for 120 min at 4°C (in accordance with the manufacturer’s recommendations) to
133 deposit the nanoparticles and separate the supernatant, which was then digested with acid
134 (HCl:HNO₃ 2:1 v/v) before ICP-OES analysis.

135

136 *Cell Culture*

137 The HaCaT cell line, a nontumorigenic immortalized human keratinocyte cell line (Boukamp et
138 al., 1988), was obtained from Cell Lines Services (Eppelheim, Germany). Cells were grown in
139 complete medium, i.e., Dulbecco’s modified Eagle’s medium, supplemented with 10% fetal
140 bovine serum (FBS), 2 mM L-glutamine, 100 U/mL penicillin, 100 μ g/mL streptomycin and 250
141 μ g/mL fungizone at 37 °C in 5% CO₂ humidified atmosphere. Cells were observed daily under
142 an inverted phase-contrast Eclipse TS100 microscope (Nikon, Tokyo, Japan). For each
143 experiment, cells were allowed to adhere for 24 h and then exposed to Cit10 or PEG10 AgNPs
144 (dispersed through vortex in cell culture medium). For the assays cells were in passage number
145 45-50. Depending on the experiment, the silver ion and the coating agent per se, dissolved in
146 complete medium, were used as controls. The effects were measured after 4, 24 and 48 h.

147

148 *Viability assay*

149 Cell viability was determined by the colorimetric 3-(4,5- dimethyl-2-thiazolyl)-2,5-diphenyl
150 tetrazolium bromide (MTT) assay, measuring intracellular reduction of tetrazolium salts into
151 purple formazan by viable cells (Twentyman and Luscombe, 1987). Cells were seeded in 96-well
152 plates at a concentration of 6×10^4 cells/mL. Fifty microliters of MTT (1 mg/mL) in phosphate
153 buffered saline (PBS) were then added to each well, and incubated for 4h at 37 °C, 5% CO₂.
154 Medium was then removed and 150 μ L of DMSO were added to each well for solubilization of
155 formazan crystals. The optical density of reduced MTT was measured at 570 nm in a microtiter
156 plate reader (Synergy HT Multi-Mode, BioTeK, Winooski, VT), and cell viability was calculated
157 as [(Sample Abs –DMSO Abs) / (Control Abs – DMSO Abs)]*100. Three independent assays
158 were performed with at least 2 technical replicates each and the results compared with the control
159 (no exposure). From our previous MTT results (Bastos et al., 2016), the IC₅₀ for 30 nm citrate

160 coated AgNPs (the most cytotoxic) was 40 mg/mL and 37.4 mg/mL at 24 and 48 h respectively.
161 Therefore, the concentrations of AgNPs corresponding to IC50 and IC20 (40 mg/mL and 10
162 mg/mL, respectively) were selected for 10 nm AgNPs assays in order to enable comparisons
163 between sizes.

164

165 *Immunofluorescence of p65 subunit of NF- κ B in human keratinocytes*

166 After the 4 h treatments with 10 and 40 μ g/mL of Cit10 or PEG 10AgNPs, coverslips were washed
167 with PBS and permeabilized with 0.2% Triton X-100 for 15 min followed by three washes with
168 PBS. Cells were treated with PBS containing BSA at a concentration of 1 mg/mL as a blocking
169 agent for 1 hour. Cells were then washed three times with PBS and treated with anti-human NF-
170 κ B antibody (p65 subunit, Santa Cruz Biotechnology, Inc. Dallas, Texas USA) diluted 1/200 in
171 PBS plus 0.5% BSA for 1 hour at room temperature. After three washes with PBS, coverslips
172 were treated with a second antibody, Alexa fluor 488 anti-rabbit IgG diluted 1:200 in PBS plus
173 0.5% BSA for 1 hour at room temperature. After three washes with PBS, coverslips were treated
174 with 0.5 μ g/ml DAPI in PBS plus 0.5% BSA for 20 seconds, washed in PBS and mounted on glass
175 microscope slides using Mowoil. Cells were imaged using confocal microscopy.

176

177 *Cytokine estimation using cytometric bead array*

178 Cytokine production was assessed using Bioplex kits. Briefly, the supernatants (collected from
179 cell viability studies, centrifuged and frozen at -80°C) were used to estimate the release of the
180 following cytokines from treated cells: interleukin-1 beta (IL-1 β), IL-6, tumour necrosis factor-
181 alpha (TNF- α), IL-10 and monocyte chemoattractant protein-1 (MCP-1). Bead array kits were
182 obtained from Beckton Dickinson (Oxford, UK) and a master mix prepared according to the
183 manufacturer's instructions. The master mix was incubated with each of the test supernatants for
184 1 h, followed by the addition of detection beads and incubated for a further 2 h at room
185 temperature. The beads were then washed in wash buffer and analysed using a BD FACSAArray™
186 flow cytometer which had previously been set up and calibrated using standard beads for each
187 cytokine under investigation.

188

189 *Statistical analysis*

190 The results are reported as mean \pm standard deviation (SD) of 2 technical replicates in each of the
191 3 independent experiments. For MTT assay, the statistical significance between control and
192 exposed cells was performed by one-way ANOVA, followed by Dunnett and Dunn's method (as
193 parametric and non-parametric test, respectively), using Sigma Plot 12.5 software (Systat
194 Software Inc.). For the other assays, results were compared using two-way ANOVA, followed by
195 Holm-Sidak test using also Sigma Plot 12.5 software (Systat Software Inc.). The differences were
196 considered statistically significant for $p < 0.05$.

197

198 **Results**

199 *Physicochemical characterization of AgNPs*

200 A summary of the physico-chemical properties of the NMs is provided in table 1. The spherical
201 shape and diameter of the AgNPs were verified by transmission electron microscopy, TEM (Fig.
202 1) and found to agree with the manufacturer information (Table 1). The wavelength of the
203 maximum absorbance peak in the UV-Vis spectra also matched the expected values. Regarding
204 the DLS assessment of hydrodynamic diameters (Dh), polydispersity indexes (PdI > 0.3)
205 indicated large variability in particle size, especially for the Cit10 NPs, hence the Z-average sizes
206 may lack accuracy. PEG10 NPs showed higher Dh than Cit10, as expected based on the larger
207 size of PEG compared to citrate. The zeta-potential values confirmed Cit10 AgNPs to have a
208 negative surface charge (ζ -34 mV), which is expected as citrate is using as a coating to prevent
209 agglomeration/aggregation through electrostatic repulsions, whereas PEG10 NPs, which are also
210 designed to stabilize NPs through steric interactions, showed a less negative surface (ζ -14 mV).
211 We have also assessed the amount of ionic silver (Ag^+) released from AgNPs, which was found
212 to be low in water (< 1%), but significantly increased when the NPs were incubated in culture
213 medium. Dissolved Ag^+ reached 14% in Cit10 suspensions after 4 h and 11 % in PEG10
214 suspensions after 24 and 48 h, this lower value likely relating to a more efficient protection of
215 PEG coating against NP surface oxidation.

216

217 *Effects on cell growth and viability*

218 HaCaT cells in control conditions (exposed to cell culture medium) showed typical morphology
219 (Figs. 2a and 3a). When cells were exposed to Cit10 and PEG10 AgNPs for 24 h (2b, 2c, 2d and
220 2e), their confluence decreased, especially at the highest concentration tested (40 $\mu\text{g}/\text{mL}$). The
221 decrease in cell confluence was more visible after 48 h (Fig. 3b, 3c, 3d and 3e). Morphologically,
222 exposed cells (to both Cit10 and PEG10 NPs) showed large precipitates/aggregates of AgNPs in
223 the medium, and confluence appeared to be, on average, lower for Cit10 exposed cells.

224 The viability of HaCaT cells was negatively affected by both types of AgNP investigated in this
225 study (Fig. 4). Relative to controls, the viability of exposed cells was significantly reduced
226 ($p < 0.05$) upon exposure to Cit10 AgNPs at 10 $\mu\text{g}/\text{mL}$ and 40 $\mu\text{g}/\text{mL}$ after 4 h, 24 h and 48 h.
227 Following PEG10 AgNP exposure, the viability of cells following exposure at a concentration of
228 10 $\mu\text{g}/\text{mL}$ was not affected at 4h but a significant reduction in cell viability was observed at 24
229 and 48 h at this concentration. At a concentration of 40 $\mu\text{g}/\text{mL}$ PEG10 NPs significantly decreased
230 cell viability at all time points (4, 24 and 48 h).

231

232 *NF- κ B activation and inflammatory cytokine release*

233 Activation of NF- κ B in HaCaT cells by AgNPs was evaluated by immunofluorescence; in its
234 inactive state NF- κ B is located in the cytoplasm, and in its active state is localized in the nucleus.
235 Figure 5 a-c shows a positive control with 240 μ M of H₂O₂ where there is a great intensity of p65
236 staining in the nucleus. Also, controls (including: cells only (no staining), cells stained with only
237 the primary antibody and samples stained with the second antibody only) were done to check the
238 autofluorescence in cells (data not shown). In control cells, most NF- κ B staining was localized in
239 the cell cytoplasm, with occasional occurrence in the nucleus. Regarding AgNP exposed cells,
240 there was no evidence of NF- κ B activation (i.e. no increase in the intensity of staining in the
241 nucleus) (Fig. 5 e-g). A decrease in p65 staining in the nucleus after exposure to 40 μ g/mL PEG10
242 AgNPs was observed comparing to control cells (Fig. 5h). To confirm the decrease in p65 staining
243 observed in Fig. 5h, a quantification of the nucleus fluorescence intensity of HaCaT microscopy
244 images were done using the ImageJ software (Fig. 5i).

245 The release of cytokines by HaCaT cells treated with AgNPs is shown in Figure 6.
246 Lipopolysaccharide (LPS) stimulated a significant increase in MCP-1 release at 48h, when
247 compared to the control. MCP-1 production significantly decreased following exposure of HaCaT
248 cells to both AgNP types and was most pronounced at a concentration of for 40 μ g/mL, compared
249 to negative and positive controls ($p < 0.001$). No effects were observed on the other cytokines
250 studied, IL-1 β , IL-6, IL-10 and TNF- α , after exposure to both AgNPs at both times (data not
251 shown).

252

253 **Discussion**

254 Citrate-coated AgNPs are among the most widely used AgNPs in multiple industrial applications
255 (Tolaymat et al., 2010), while the less used PEG-coated AgNPs have gained increasing attention
256 over recent years by, for instance, the biomedical industry due to their high stability and reduced
257 reactivity (Brandenberger et al., 2010; Ginn et al., 2014; Ryan et al., 2008; Thorley and Tetley,
258 2013). Therefore, there is need to better understand the influence of coatings of the biological
259 effects of NPs, and in particular the inflammatory responses. As skin represents one of the major
260 organs in contact with AgNPs, we compared the viability and inflammatory responses induced
261 by citrate or PEG-coated AgNPs with a core diameter of 10 nm (Cit10 and PEG10 AgNPs) in
262 human epidermis keratinocytes (HaCaT cells).

263 From the cytotoxicity results, Cit10 AgNPs were more toxic than PEG10 NPs. The higher toxicity
264 of Cit10 AgNPs was particularly relevant for low doses, since a lower concentration (10 μ g/mL)
265 of Cit0 NPs induced a statistically significant decrease in cell viability 4h post exposure, that was
266 not evident for PEG AgNPs. At higher doses (40 μ g/mL) and exposure periods, PEG10 and Cit10
267 AgNPs reduced viability in similar ways. These data suggest that, for these skin cells, the
268 influence of coating is more important at low AgNP concentrations, whereas by increasing
269 concentration, the influence of coating seems to be less relevant. A significant decrease in BEAS-

270 2B (bronchial epithelial) cell viability upon exposure to 20 nm citrate-coated AgNPs at 6.25-50
271 $\mu\text{g}/\text{mL}$ after 24 h has been observed previously (Wang et al., 2014). Also, Song et al. (2012)
272 showed a decrease on cell viability in human liver cell line - HL-7702 after exposure to PEG-
273 coated AgNPs in dose- and time-dependent manner at doses from 6.25 $\mu\text{g}/\text{mL}$. Future studies
274 could assess the sensitivity of different cell types to the AgNPs used in this study.

275 A complex interplay between environmental and genetic factors control immune system
276 responses and when a deregulation of immune homeostasis occurs, host defense can be impaired
277 and at the same time cause excessive and potential harmful inflammatory responses, which could
278 be responsible for several immune disorders (Bieber, 2008; Morar et al., 2006). The ability of
279 NPs to elicit pro-inflammatory responses is frequently assessed in *in vitro* and *in vivo* studies as
280 a marker of their toxicity (eg, Schoemaker et al., (2002)). Thus, understanding NP-dependent
281 regulation of cytokine production is essential, since this process conditions shifts from acute to
282 chronic phases of allergic inflammation (Rossi and Zlotnik, 2000). NF- κB pathways have been
283 traditionally associated to increases in the production of inflammatory cytokines which could be
284 implicated in the development of a variety of diseases (Driscoll et al., 1997; Mossman and Churg,
285 1998). AgNPs did not activate NF- κB in HaCaT cells in this study. In fact, NF- κB may be
286 inhibited after exposure to the higher concentration (40 $\mu\text{g}/\text{mL}$) of PEG10 AgNPs. It is described
287 in literature that the inhibition or absence of NF- κB activation induces apoptosis or sensitizes cells
288 to apoptosis (Schoemaker et al., 2002).

289 Murray et al (2013) found that a co-exposure of human epidermal keratinocytes (HEK cells) to
290 superparamagnetic iron oxide (SPION) nanoparticles and UVB induced NF- κB activation and
291 release of inflammatory mediators such as the cytokines IL-6 and IL-8. Carbon black NPs have
292 also been demonstrated to induce NF- κB activation in macrophages to stimulate TNF α production
293 (Brown et al., 2004). However, it has also been recognized that NF- κB signaling has important
294 functions in the maintenance of physiological immune homeostasis, particularly in epithelial cells
295 (Wullaert et al., 2011). In a previous work (Bastos et al., 2016), we have demonstrated, by
296 Annexin-V/PI assay and expression of genes involved in apoptosis, that Cit30 AgNPs induced
297 preferably necrotic pathways, while cells exposed to PEG30 AgNPs stimulated increases of cells
298 in earlier phase of apoptosis (therefore a more reversible process) and no necrosis, supporting that
299 coating conditions how these AgNPs influence the cell apoptosis/necrosis pathways. A major role
300 of NF- κB pathways involve the regulation of anti-apoptotic genes, by NF- κB directly binding and
301 inhibiting CASP3, -7 and -9 which seems to be happening in citrate- AgNPs exposed cells
302 (Schoemaker et al., 2002). Considering that only PEG10 AgNPs inhibit NF- κB , we therefore
303 hypothesize that this may be involved in the induction of apoptosis by activating CASP3 found
304 in PEG30-exposed cells versus Cit30-exposed ones. In the future we suggest that NF- κB
305 activation/inhibition may be used to a greater extent when assessing the hazard of coating and
306 AgNPs to better understand the mechanisms (i.e. cellular and molecular events) underlying their

307 toxicity. On the other hand, Brown et al (2004) showed that ultrafine carbon black particles
308 (UfCB)-induced nuclear translocation of NF- κ B in human monocytes which occurs through ROS-
309 mediated mechanism. Indeed, in our previous study 30 nm citrate- and PEG- AgNPs induced a
310 significant increase in the production of ROS by HaCaT cells at the highest dose tested (40
311 μ g/mL), compared to control cells. However, the ROS levels were similar for both NP types which
312 do not explain the NF- κ B inhibition by PEG10 AgNPs. Thus, for further studies we also suggest
313 the quantification of NF- κ B activation (e.g. by western blotting) and determination of ROS
314 production.

315 Concerning cytokine release, neither Cit10 nor PEG10 AgNPs induced IL-1 β , IL-6, IL-10, TNF-
316 α and MCP-1 production by HaCaT cells. Instead, compared to control cells, they decreased
317 MCP-1 production after 48 h exposure, this reduction being more pronounced at the higher
318 concentration (40 μ g/mL), while the control cells presented an increase of this cytokine as already
319 described by Takahashi et al (1995) who reported values close to ours for monocytes and
320 endothelial cells *in vitro*. The information regarding the influence of AgNPs on the stimulation of
321 these cytokines from keratinocytes release is scarce, and sometimes contradictory, as different
322 exposure conditions, concentrations, coating, cell type, NP size and synthesis have been
323 considered in the literature (Abbott Chalew and Schwab, 2013; Giovanni et al., 2015; Miethling-
324 Graff et al., 2014; Orłowski et al., 2013; Samberg et al., 2010; Suliman Y et al., 2013a; Wong et
325 al., 2009; Yen et al., 2009). For instance, Orłowski and co-workers (2013) found an increase of
326 MCP-1 production in murine keratinocytes (murine 291.03C) and by monocytes (RAW 264.7)
327 after exposure to unmodified AgNPs. Also, human umbilical vein endothelial (HUVEC) cells
328 showed a significant increase of IL-6, IL-8 and MCP-1 at doses higher than 1 mg/L AgNPs (Shi
329 et al., 2014). Moreover, confirming the inflammatory potential of AgNPs, several interleukins
330 and TNF- α were reported to increase upon exposure of HEK cells (Samberg et al., 2010) and
331 macrophages (Yen et al., 2010) to AgNPs. On the other hand, several authors reported an
332 undetectable stimulation of cytokines in response to metal NPs, as observed in the present study.
333 For example, Murray et al (2013) demonstrated that HEK cells exposed to superparamagnetic
334 iron oxide nanoparticles maintained the IL-1 β , IL-10 and TNF- α below detectable levels (while
335 increasing IL-6); and also that mouse epidermal cells (JB6 P+) maintained INF- γ and IL-12 below
336 the detectable levels after exposure to the same nanoparticles. Similarly, Samberg et al (2010) did
337 not find detectable levels of IL-10 in HEK cells exposed to unwashed AgNPs. In mice peritoneal
338 tissues and in RAW cells, Wong et al (2009) demonstrated that AgNPs have an anti-inflammatory
339 effect decreasing TNF- α , and INF- γ . Also, Parnsamut and Brimson (2015) found that AgNPs
340 inhibited TNF- α expression in leukemic cell lines. It is known that cytokines can adsorb onto the
341 surface of particles, which may compromise their detection (Brown et al., 2010). Thus, it should
342 not be excluded that AgNPs may induce cytokine production by keratinocytes but that the
343 cytokines bind to the AgNP surface to prevent their detection. How proteins bind to nanoparticles

344 is currently an important topic of debate. For example, Deng et al (2013) showed that human
345 plasma proteins differently bind to positively and negatively charged polymer-coated gold NPs,
346 which elicited different biological responses, and that only the negatively charged nanoparticles
347 induced cytokine release from THP-1 cells. While proteins can bind to different nanoparticles,
348 the biological outcome may not be the same. Selection of cytokines for assessment in this study
349 was prioritized based on the outcome of a literature search which identified cytokines that are
350 commonly produced following exposure of cells to NPs. Future studies could therefore assess a
351 wider panel of cytokines.

352 In summary, our study demonstrated that while citrate- and PEG-coated AgNPs decreased the
353 viability of HaCaT cells. Citrate coated AgNPs were more cytotoxic than PEG coated NPs,
354 particularly at low concentrations and shorter incubation times. At higher AgNPs concentration,
355 the influence of coating became less relevant. Also, we demonstrated that, independent of the
356 coating, AgNPs did not induce cytokine production, and decreased MCP-1 release. Finally,
357 PEG10 AgNPs at high concentrations inactivated the transcription factor NF- κ B, and putative
358 correlation with anti-inflammatory and anti-apoptotic homeostasis should be further explored.

359

360 **Competing interests**

361 The authors declare that they have no competing interests.

362

363 **Acknowledgments**

364 This work was developed in the scope of the projects CICECO-Aveiro Institute of Materials (Ref.
365 FCT UID/CTM/50011/2013) and CESAM (Ref. FCT UID/AMB/50017/2013), financed by
366 national funds through the FCT/MEC and when applicable co-financed by the European Regional
367 Development Fund (FEDER) under the PT2020 Partnership Agreement. Funding to the project
368 FCOMP-01-0124-FEDER-021456 (Ref. FCT PTDC/SAU-TOX/120953/2010) by FEDER
369 through COMPETE and by national funds through FCT, and the FCT-awarded grants
370 (SFRH/BD/81792/2011; SFRH/BPD/111736/2015) are acknowledged. I.F.D and A.L.D.S.
371 acknowledge FCT/MCTES for the research contracts under the Program ‘Investigador FCT’
372 2014.

373

374 **References**

- 375 Abbott Chalew TE, Schwab KJ (2013) Toxicity of commercially available engineered
376 nanoparticles to Caco-2 and SW480 human intestinal epithelial cells. *Cell Biol Toxicol*
377 29(2):101-116.
- 378 Abdelhalim MAK, Jarrar BM (2011) Renal tissue alterations were size-dependent with smaller
379 ones induced more effects and related with time exposure of gold nanoparticles. *Lipids Health*
380 *Dis* 10(1):1.
- 381 Ahlberg S, Meinke MC, Werner L, Epple M, Diendorf J, Blume-Peytavi U, Lademann J, Vogt A,
382 Rancan F (2014) Comparison of silver nanoparticles stored under air or argon with respect to
383 the induction of intracellular free radicals and toxic effects toward keratinocytes. *Eur J Pharm*
384 *Biopharm* 88(3):651-657
- 385 Bastos V, de Oliveira JF, Brown D, Jonhston H, Malheiro E, Daniel-da-Silva AL, Duarte IF,
386 Santos C, Oliveira H (2016) The influence of Citrate or PEG coating on silver nanoparticle
387 toxicity to a human keratinocyte cell line. *Toxicol Lett* 249:29-41.
- 388 Behra R, Sigg L, Clift M, Herzog F, Minghetti M, Johnston B, Petri-Fink A, Rothen-Rutishauser
389 B (2013) Bioavailability of silver nanoparticles and ions: from a chemical and biochemical
390 perspective. *J R Soc Interface* 10(87):20130396.
- 391 Benn T, Westerhoff P (2008) Nanoparticle silver released into water from commercially available
392 sock fabrics. *Environ Sci Technol* 42(11):4133-4139 .
- 393 Bieber T (2008) Atopic dermatitis. *N Engl J Med* 358 (14):1483-1494.
- 394 Boonkaew B, Kempf M, Kimble R, Cuttle L (2014) Cytotoxicity testing of silver-containing burn
395 treatments using primary and immortal skin cells. *Burns* 40(8):1562-1569.
- 396 Brandenberger C, Mühlfeld C, Ali Z, Lenz A-GG, Schmid O, Parak WJ, Gehr P, Rothen-
397 Rutishauser B (2010) Quantitative evaluation of cellular uptake and trafficking of plain and
398 polyethylene glycol-coated gold nanoparticles. *Small* 6(15):1669-1678.
- 399 Brown DM, Dickson C, Duncan P, Al-Attili F, Stone V (2010) Interaction between nanoparticles
400 and cytokine proteins: impact on protein and particle functionality. *Nanotechnology*
401 21(21):215104.
- 402 Brown DM, Donaldson K, Borm PJ, Schins RP, Dehnhardt M, Gilmour P, Jimenez LA, Stone V
403 (2004) Calcium and ROS-mediated activation of transcription factors and TNF-alpha cytokine
404 gene expression in macrophages exposed to ultrafine particles. *Am J Physiol Lung Cell Mol*
405 *Physiol* 286(2):L344-L353.
- 406 Caballero-Díaz E, Pfeiffer C, Kastl L, Gil P, Simonet B, Valcárcel M, Lamana J, Laborda F, Parak
407 WJ (2013) The toxicity of silver nanoparticles depends on their uptake by cells and thus on
408 their surface chemistry. *Part Part Syst Charact* 30(12):1079-1085.

409 Comfort KK, Maurer EI, Hussain SM, (2014) Slow release of ions from internalized silver
410 nanoparticles modifies the epidermal growth factor signaling response.
411 *Colloids Surf B Biointerfaces* 123:136-142.

412 Deng ZJ, Liang M, Toth I, Monteiro M, Minchin RF (2013) Plasma protein binding of positively
413 and negatively charged polymer-coated gold nanoparticles elicits different biological
414 responses. *Nanotoxicology* 7(3):314-322.

415 Driscoll KE, Carter JM, Hassenbein DG (1997) Cytokines and particle-induced inflammatory cell
416 recruitment. *Environ Health Perspect* 105(Suppl 5):1159.

417 Eckhardt S, Brunetto P, Gagnon J, Priebe M, Giese B, Fromm K (2013) Nanobio silver: its
418 interactions with peptides and bacteria, and its uses in medicine. *Chem Rev* 113(7):4708-4754.

419 EPA, EPA (2010) State of the Science Literature Review: Everything Nanosilver and More.
420 Scientific, Technical, Research, Engineering and Modeling Support Final Report.

421 Fujiwara N, Kobayashi K (2005) Macrophages in inflammation.
422 *Curr Drug Targets Inflamm Allergy* 4(3):281-286.

423 George R, Merten S, Wang TT, Kennedy P, Maitz P (2014) In vivo analysis of dermal and
424 systemic absorption of silver nanoparticles through healthy human skin. *Australas J Dermatol*
425 55(3):185-190.

426 Ginn C, Khalili H, Lever R, Brocchini S (2014) PEGylation and its impact on the design of new
427 protein-based medicines. *Future Med Chem* 6(16):1829-1846.

428 Giovanni M, Yue J, Zhang L, Xie J, Ong CN (2015) Pro-Inflammatory Responses of RAW264. 7
429 Macrophages when Treated with Ultralow Concentrations of Silver, Titanium Dioxide, and
430 Zinc Oxide Nanoparticles. *J Hazard Mater* 297:146-152.

431 Graves JD, Craxton A, Clark EA (2004) Modulation and function of caspase pathways in B
432 lymphocytes. *Immunol Rev* 197(1):129-146.

433 Kelso A (1998) Cytokines: principles and prospects. *Immunol Cell Biol* 76(4), 300-317.

434 Kim TH, Kim M, Park HS, Shin US, Gong MS, Kim HW (2012) Size-dependent cellular toxicity
435 of silver nanoparticles. *J Biomed Mater Res A* 100(4):1033-1043.

436 Larese FF, D'Agostin F, Crosera M, Adami G, Renzi N, Bovenzi M, Maina G (2009) Human skin
437 penetration of silver nanoparticles through intact and damaged skin. *Toxicology* 255(1):33-37.

438 Lu W, Senapati D, Wang S, Tovmachenko O, Singh A, Yu H, Ray P (2010) Effect of Surface
439 Coating on the Toxicity of Silver Nanomaterials on Human Skin Keratinocytes. *Chem Phys*
440 *Lett* 487(1):92-96.

441 Miethling-Graff R, Rumpker R, Richter M, Verano-Braga T, Kjeldsen F, Brewer J, Hoyland J,
442 Rubahn H-GG, Erdmann H (2014) Exposure to silver nanoparticles induces size- and dose-
443 dependent oxidative stress and cytotoxicity in human colon carcinoma cells. *Toxicol In*
444 *Vitro* 28(7):1280-1289.

445 Morar N, Willis-Owen SAG, Moffatt MF (2006) The genetics of atopic dermatitis. *J Allergy Clin*
446 *Immun* 118(1):24-34.

447 Mossman BT, Churg A (1998) Mechanisms in the pathogenesis of asbestosis and silicosis. *Am J*
448 *Respir Crit Care Med* 157(5):1666-1680.

449 Murray AR, Kisin E, Inman A, Young S-H, Muhammed M, Burks T, Uheida A, Tkach A, Waltz
450 M, Castranova V (2013) Oxidative stress and dermal toxicity of iron oxide nanoparticles in
451 vitro. *Cell Biochem Biophys* 67(2):461-476.

452 Noursadeghi M, Tsang J, Haustein T, Miller RF, Chain BM, Katz DR (2008) Quantitative imaging
453 assay for NF-kappaB nuclear translocation in primary human macrophages. *J*
454 *Immunol Methods* 329(1):194-200.

455 Nowack B, Bucheli T (2007) Occurrence, behavior and effects of nanoparticles in the
456 environment. *Environ Pollut* 150(1):5-22.

457 Nowack B, Krug H, Height M (2011) 120 years of nanosilver history: implications for policy
458 makers. *Environ Sci Technol* 45(4):1177-1183.

459 Orłowski P, Krzyzowska M, Zdanowski R, Winnicka A, Nowakowska J, Stankiewicz W,
460 Tomaszewska E, Celichowski G, Grobelny J (2013) Assessment of in vitro cellular responses
461 of monocytes and keratinocytes to tannic acid modified silver nanoparticles. *Toxicol in*
462 *Vitro* 27(6):1798-1808.

463 Pang C, Brunelli A, Zhu C, Hristozov D, Liu Y, Semenzin E, Wang W, Tao W, Liang J, Marcomini
464 A, et al (2015) Demonstrating approaches to chemically modify the surface of Ag nanoparticles
465 in order to influence their cytotoxicity and biodistribution after single dose acute intravenous
466 administration. *Nanotoxicology* 1-11.

467 Park E-JJ, Choi K, Park K (2011a) Induction of inflammatory responses and gene expression by
468 intratracheal instillation of silver nanoparticles in mice. *Arch Pharm Res* 34(2):299-307.

469 Park J, Lim D-HH, Lim H-JJ, Kwon T, Choi J-sS, Jeong S, Choi I-HH, Cheon J (2011b) Size
470 dependent macrophage responses and toxicological effects of Ag nanoparticles. *Chem*
471 *Commun (Camb)* 47(15):4382-4384.

472 Parnsamut C, Brimson S (2015) Effects of silver nanoparticles and gold nanoparticles on IL-2, IL-
473 6, and TNF- α production via MAPK pathway in leukemic cell lines. *Genet Mol*
474 *Res* 14(2):3650.

475 Rossi D, Zlotnik A (2000) The biology of chemokines and their receptors. *Annu Rev*
476 *Immunol* 18(1):217-242.

477 Ryan SMM, Mantovani G, Wang X, Haddleton DM, Brayden DJ (2008) Advances in PEGylation
478 of important biotech molecules: delivery aspects. *Expert Opin Drug Deliv* 5(4):371-383.

479 Samberg ME, Oldenburg SJ, Monteiro-Riviere NA (2010) Evaluation of Silver Nanoparticle
480 Toxicity in Skin in Vivo and Keratinocytes in Vitro. *Environ Health Perspect* 118(3):407.

481 Schinwald A, Murphy F, Prina-Mello A, Poland C, Byrne F, Movia D, Glass J, Dickerson JC,
482 Schultz DA, Jeffree CE, Macnee W, Donaldson K (2012) The threshold length for fibre-
483 induced acute pleural inflammation: shedding light on the early events in asbestos-induced
484 mesothelioma. *Toxicol Sci* 128(2):461-70.

485 Schoemaker MH, Ros JE, Homan M, Trautwein C (2002) Cytokine regulation of pro-and anti-
486 apoptotic genes in rat hepatocytes: NF- κ B-regulated inhibitor of apoptosis protein 2 (cIAP2)
487 prevents apoptosis. *J Hepatol* 36(6):742-750.

488 Sharma V, Yngard R, Lin Y (2009) Silver nanoparticles: green synthesis and their antimicrobial
489 activities. *Adv Colloid Interface Sci* 145(1):83-96.

490 Shi J, Sun X, Lin Y, Zou X, Li Z, Liao Y, Du M, Zhang H (2014) Endothelial cell injury and
491 dysfunction induced by silver nanoparticles through oxidative stress via IKK/NF- κ B pathways.
492 *Biomaterials* 35(24):6657-6666.

493 Suliman YA, Ali D, Alarifi S, Harrath A, Mansour L, Alwasel S (2013a) Evaluation of cytotoxic,
494 oxidative stress, proinflammatory and genotoxic effect of silver nanoparticles in human lung
495 epithelial cells. *Environ Toxicol* 30(2):149-160.

496 Suliman YAO, Ali D, Alarifi S, Harrath AH, Mansour L, Alwasel SH (2013b) Evaluation of
497 cytotoxic, oxidative stress, proinflammatory and genotoxic effect of silver nanoparticles in
498 human lung epithelial cells. *Environ Toxicol* 30(2):149-160.

499 Takahashi M, Masuyama JI, Ikeda U, Kasahara T, Kitagawa SI, Takahashi YI, Shimada K, Kano
500 S (1995) Induction of monocyte chemoattractant protein-1 synthesis in human monocytes
501 during transendothelial migration in vitro. *Circ Res* 76(5):750-757.

502 Tejamaya M, Römer I, Merrifield R, Lead J (2012) Stability of citrate, PVP, and PEG coated silver
503 nanoparticles in ecotoxicology media. *Environ Sci Technol* 46(13), 7011-7017.

504 Thorley AJ, Tetley TD (2013) New perspectives in nanomedicine. *Pharmacol Therapeut*
505 140(2):176-185.

506 Tolaymat TM, El Badawy AM, Genaidy A, Scheckel KG, Luxton TP, Suidan M (2010) An
507 evidence-based environmental perspective of manufactured silver nanoparticle in syntheses
508 and applications: a systematic review and critical appraisal of peer-reviewed scientific papers.
509 *Sci Total Environ* 408(5):999-1006.

510 Twentyman P, Luscombe M (1987) A study of some variables in a tetrazolium dye (MTT) based
511 assay for cell growth and chemosensitivity. *Br J Cancer* 56(3):279.

512 Vance ME, Kuiken T, Vejerano EP, McGinnis SP, Hochella Jr MF, Rejeski D, Hull, MS (2015)
513 Nanotechnology in the real world: Redeveloping the nanomaterial consumer products
514 inventory. *Beilstein J Nanotechnol* 6(1):1769-1780.

515 Wang X, Ji Z, Chang C, Zhang H, Wang M, Liao Y-P, Lin S, Meng H, Li R, Sun B, et al (2014)
516 Use of coated silver nanoparticles to understand the relationship of particle dissolution and
517 bioavailability to cell and lung toxicological potential. *Small* 10(2):385-398.

518 Wong KK, Cheung SO, Huang L, Niu J, Tao C, Ho C-MM, Che C-MM, Tam PK (2009) Further
519 evidence of the anti-inflammatory effects of silver nanoparticles. *ChemMedChem* 4(7):1129-
520 1135.

521 Wullaert A, Bonnet MC, Pasparakis M (2011) NF- κ B in the regulation of epithelial homeostasis
522 and inflammation. *Cell Res* 21(1):146-158.

523 Yang E-JJ, Jang J, Lim D-HH, Choi I-HH (2012) Enzyme-linked immunosorbent assay of IL-8
524 production in response to silver nanoparticles. *Methods Mol Biol* 131-139.

525 Yarin AA, Belyakov IM (2004) Cytokines in the thymus: production and biological effects. *Curr*
526 *Med Chem* 11(4):447-464.

527 Yen H-J, Hsu S-H, Tsai C-L (2009) Cytotoxicity and immunological response of gold and silver
528 nanoparticles of different sizes. *Small* 5(13):1553-1561.

529 Yoshizumi M, Nakamura T, Kato M, Ishioka T, Kozawa K, Wakamatsu K, Kimura H (2008)
530 Release of cytokines/chemokines and cell death in UVB-irradiated human keratinocytes,
531 HaCaT. *Cell Biol Int* 32(11):1405-1411.

532 Zhang LW, Yu WW, Colvin VL, Monteiro-Riviere NA (2008) Biological interactions of quantum
533 dot nanoparticles in skin and in human epidermal keratinocytes. *Toxicol Appl*
534 *Pharmacol* 228(2):200-211.

535

536 **Fig. 1** Transmission electron microscopy (TEM) images of Cit10 and PEG10 AgNPs used in this
537 work

538

539 **Fig. 2** Light microscopy images (100X) of HaCaT cells exposed to 10 nm citrate- AgNPs or PEG-
540 AgNPs (Cit10 or PEG10) for 24 h. a) 0 (control); b) Cit10, 10 μ g/mL; c) Cit10, 40 μ g/mL; d)
541 PEG10, 10 μ g/mL; and e) PEG10, 40 μ g/mL. Bar corresponds to 100 μ m

542

543 **Fig. 3** Light microscopy images (100X) of HaCaT cells exposed to 10 nm citrate- AgNPs or PEG-
544 AgNPs (Cit10 or PEG10) for 48 h. a) 0 (control); b) Cit10, 10 μ g/mL; c) Cit10, 40 μ g/mL; d)
545 PEG10, 10 μ g/mL; and e) PEG10, 40 μ g/mL. Bar corresponds to 100 μ m

546

547 **Fig. 4** Relative cell viability (%) of HaCaT cells after exposure to 10 and 40 μ g/mL of 10 nm
548 citrate- AgNPs or PEG- AgNPs (Cit10 or PEG10), measured by MTT assay, at 4, 24 and 48 h
549 post exposure. Data expressed as mean and standard deviation (n = 3). * indicate significant
550 differences between control at p < 0.05

551

552 **Fig. 5** Microscopy images of HaCaT cells. a) - c) are fluorescence microscopy images (400X) of
553 immunofluorescence of HaCaT cells treated with anti NF- κ B p65 antibody after stimulation with
554 240 μ M H₂O₂ for 10 min prior fixation: a) p65 subunit of NF- κ B (alexa fluor 488 anti-rabbit IgG);

555 b) DAPI staining the nucleus; c) Overlap of a and b images. d) - h) are confocal microscopy
556 images of immunofluorescence of p65 subunits of NF- κ B in human HaCaT keratinocytes exposed
557 to AgNPs for 4 h: d) 0 (control); e) 10 μ g/mL of Cit10; f) 40 μ g/mL of Cit10; g) 10 μ g/mL of
558 PEG10; h) 40 μ g/mL of PEG10. Bar corresponds to 100 μ m. i) is the quantification of the nucleus
559 fluorescence intensity of HaCaT microscopy images presented in Fig.4h using the ImageJ
560 software. Data expressed the mean and standard deviation. ** indicate significant differences
561 between control at $p < 0.01$

562

563 **Fig. 6** Cytokine release by HaCaT cells after 24 and 48h exposure to 10 nm citrate- or PEG-
564 AgNPs (Cit10 or PEG10). Control + is a positive control by adding LPS to cells. Data represent
565 the mean \pm standard deviation ($n = 3$) of the concentration (pg /ml) of MCP-1 cytokine released
566 from the cells after NPs treatment

567

568

569

570

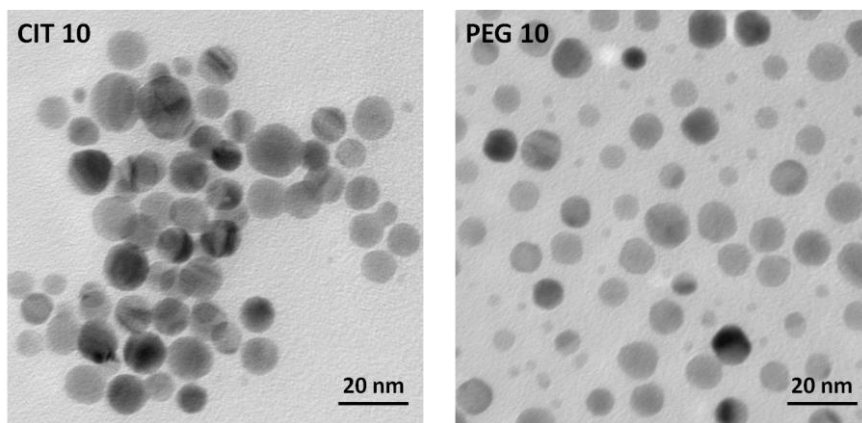


Figure 1

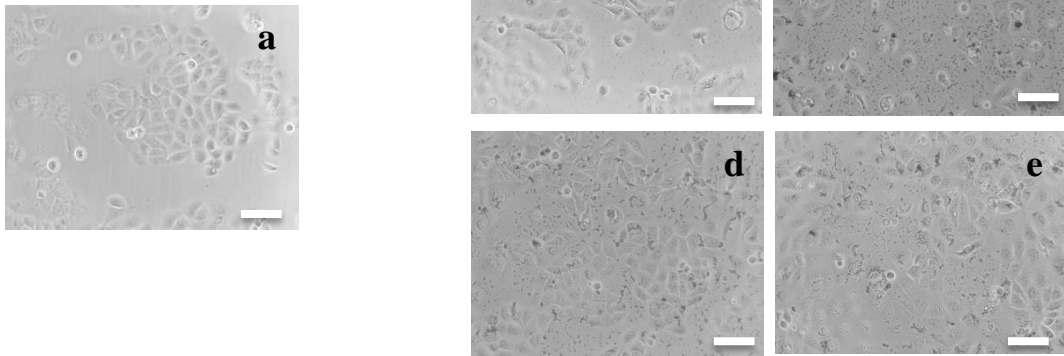


Figure 2

573

574

575

576

577

578

579

580

581

582

583

584

585

586

587

588

589

590

591

592

593

594

595

596

597

598

599

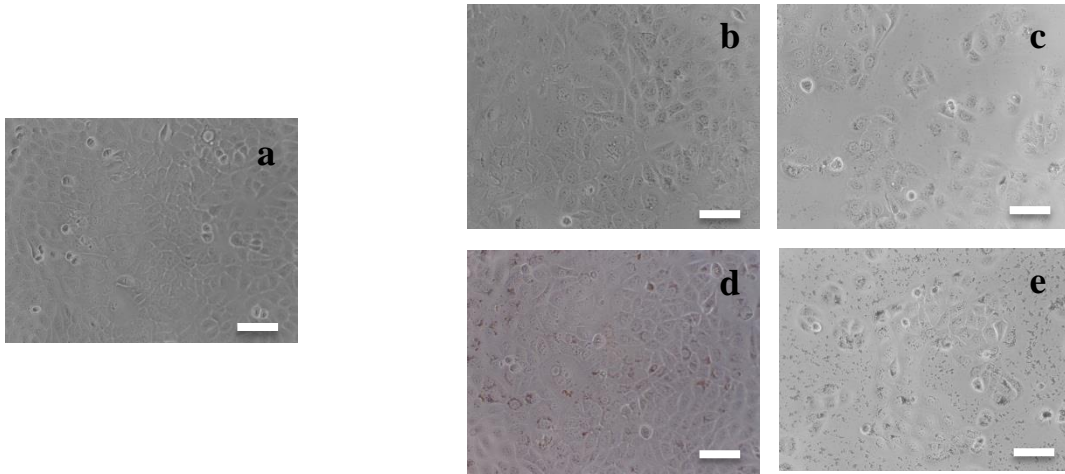


Figure 3

600
601
602
603
604
605
606
607
608
609
610
611
612
613
614
615
616
617
618
619
620
621
622
623
624
625
626
627

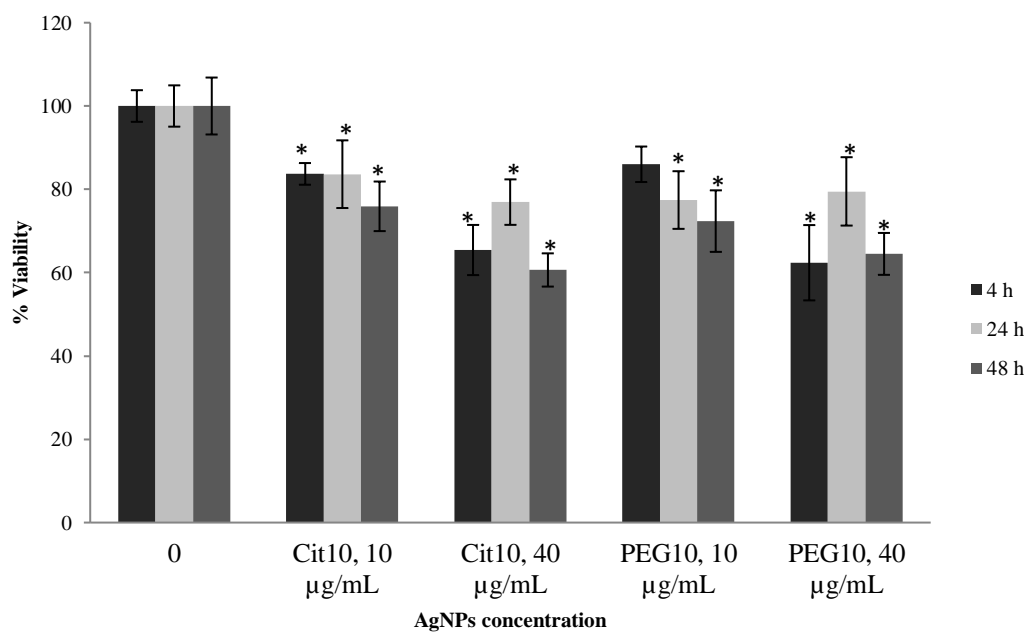


Figure 4

628
629
630
631
632
633
634
635
636
637
638
639
640
641
642
643
644
645
646
647
648
649
650
651
652
653
654
655

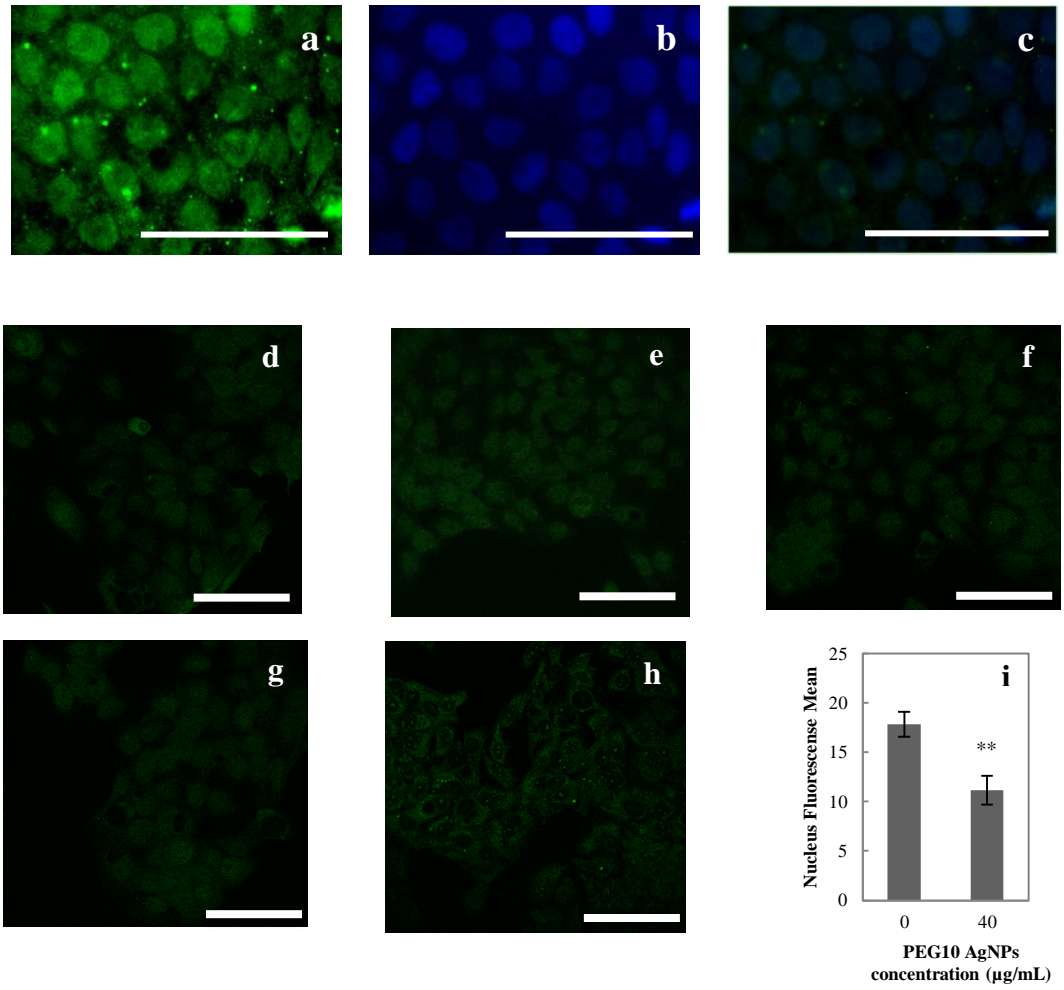


Figure 5

656
657
658
659
660
661
662
663
664
665
666
667
668
669
670

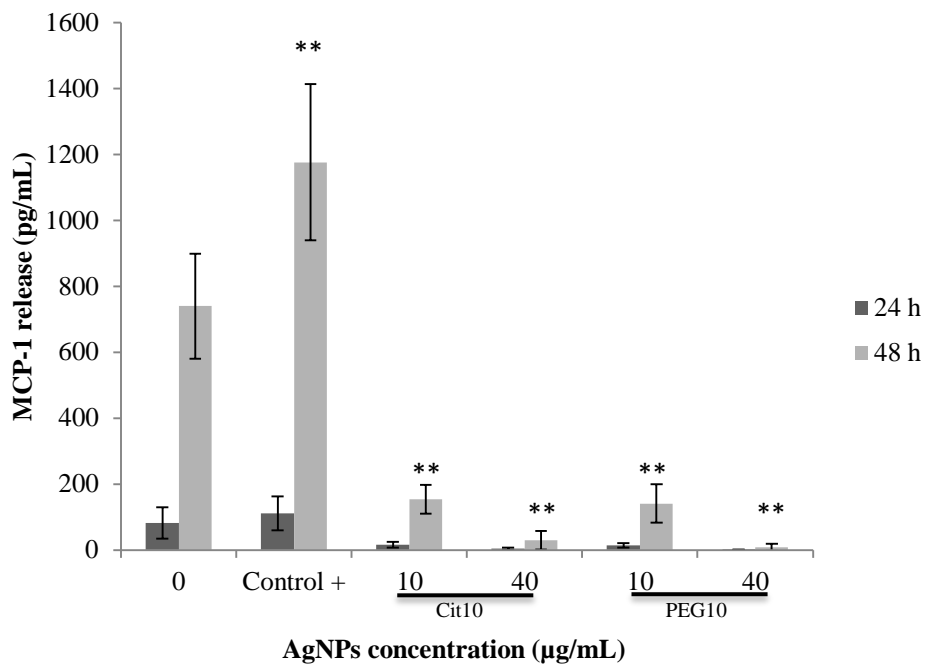


Figure 6